Principal Component Analysis of Wide Area Phasor Measurements for Islanding Detection – A Geometric View

Principal Component Analysis of Wide Area Phasor Measurements for Islanding Detection — A Geometric View

X. Liu, *Member, IEEE,* D. M. Laverty, *Member, IEEE,* R. J. Best, *Member, IEEE,*
K. Li, *Senior Member, IEEE,* D. J. Morrow, *Member, IEEE,* S. McLoone, *Senior Member, IEEE*

***Abstract*—This paper presents a new technique for the detection of islanding conditions in electrical power systems. This problem is especially prevalent in systems with significant penetrations of distributed renewable generation. The proposed technique is based on the application of principal component analysis (PCA) to data sets of wide-area frequency measurements, recorded by phasor measurement units. The PCA approach was able to detect islanding accurately and quickly when compared with conventional RoCoF techniques, as well as with the frequency difference and change of angle difference methods recently proposed in the literature. The reliability and accuracy of the proposed PCA approach is demonstrated using a number of test cases, which consider both islanding and non-islanding events. The test cases are based on real data, recorded from several phasor measurement units located in the UK power system.**

***Index Terms*—Wide area monitoring, islanding detection, reclosure, multivariate statistics, synchronized phasor measurements**

I. Introduction

GENERATION from renewable energy sources is a key component in the worldwide strategy to reduce carbon emissions and to maintain a secure and sustainable energy supply. In Northern Ireland, for example, a target has been set to achieve as high as 40% of its electricity consumption from renewable sources by 2020 [1]. A similar target has also been set by the Republic of Ireland and several other European countries, while the U.S. and China both set a target of around 20% [2]. The integration of significant quantities of distributed renewable generation into the electricity grid, however, has raised serious concerns about its potential impacts on the safe operation and stability of the grid. In this context the issue of islanding detection in the distribution power system presents great challenges, and it is going through a period of renewed interest in both industry and academia.

Islanding is a phenomenon where distributed generators (e.g. photovoltaic, wind turbines) continue operating and energizing the local loads even though they are isolated from the rest of the utility source [3], [4]. This islanding condition is particularly dangerous; if not detected it may endanger maintenance personnel. In addition, unsynchronized reconnection of an island to the main power grid may cause severe damage to the utility, the distributed generators and other customer equipment. Therefore, it is important to be able to detect islanding conditions accurately and quickly.

To achieve this, various islanding-detection techniques have been proposed [4], [5], [6]. A detailed review of these techniques has been carried out in [7]. The techniques may be described as local or remote (communication-based) approaches.

Local approaches, can be classified into passive and active methods. Passive methods based on rate-of-change of frequency (RoCoF) [3], rate of change of power [8], rate of change of frequency over power [9], vector shift [3], and harmonic impedance estimation techniques [10] have attracted wide spread attention. The most popular RoCoF relay, however, might become unsuccessful if the power imbalance in the islanded system is less than 15% [5]. Moreover, in systems with a high penetration of renewable generation there is an increased risk of false detection during load or generation trip events. Active methods perform islanding detection by injecting a disturbing signal to break the power balance [11]. For example, in the active frequency drift method, a forced change of frequency approach, the frequency of the voltage is forced to drift up or down in the island [12]. Such approaches has become mandatory for islanding prevention with solar PV in some countries. Active methods tend to have a smaller non-detection zone compared to passive methods, but have the disadvantage of often degrading power quality to a certain degree.

Classification-based passive techniques, based on fuzzy-rules [5], wavelet-transforms [4], probabilistic neural networks [13], support vector machines [13], Bayesian methods [6], and decision trees [14], [15], have been recently proposed for islanding detection in the literature. Unfortunately, investigations of these approaches have been limited to studies on simulated power systems, due to their critical demand for large volumes of historic event data. Moreover, the response time for islanding detection based on these approaches is not discussed in most studies.

Remote techniques, such as power line signalling and transfer trip schemes, usually rely on communication signals for islanding detection. Some new remote or communication-based techniques, especially PMU-based, have attracted great attention in both industry and academia in recent years. Moreover, deployment cost of these techniques is gradually redeemed by their technical good performance [16]. However, remote techniques utilized to date often focus on the distributed generator side, and in general cannot provide a real-time wide-

X. Liu, D. M. Laverty, R. J. Best, K. Li, D. J. Morrow and S. McLoone are with the School of Electronics, Electrical Engineering and Computer Science, Queen's University Belfast, Belfast, BT9 5AH, U.K. e-mail: x.liu@qub.ac.uk.

area view of the islanding situation, or produce alarming for system operators [17]. This is particularly important in systems with high penetrations of renewable generation, which can become vulnerable to nuisance tripping of islanding protection. To address this problem, reference [17] has recently proposed a PMU-based method, using a frequency difference and the change of angle difference approach. Despite the reported success of this method in several real cases, a number of outstanding problems still remain:

1) It requires a number of parameters to be determined and optimized to define the tripping time criteria for islanding detection. These parameters include thresholds for the frequency and the angle deviations and three settings for the timer. These were originally set based on experience by the authors.
2) Its response time for islanding detection is over 3 seconds, which exceeds the IEEE standard 1547-2003 [18] where the anti-islanding relay must immediately disconnect the distributed generator within 2 seconds of the formation of an island. The requirement for a response time of under 2 seconds is also defined in the IEC 61727 standard for PV systems [19].
3) Some issues may arise with the proposed islanding detection approach owing to its critical dependence on the reference frequency and reference phase angle.

This paper attempts to address these problems using an intelligent multivariate statistical approach, relying on principal component analysis (PCA) of the measurements from PMUs. This is a challenging proposition because (i) the observed phasor measurements are influenced by random load fluctuations that continuously perturb the system equilibrium slightly and in a non-stationary manner [20]; (ii) other power system events such as generator trips, line trips, and loss of load also create perturbations in the voltage, frequency, and angles similar to those generated by islanding events; (iii) the signal-to-noise ratio of PMU data is often low, making detection of islanding difficult.

Because of its simplicity, PCA, a data-driven multivariate projection-based technique, has gained great attention for monitoring complex processes, such as those found in the chemical industry [21]. PCA exploits the correlation within the typically large number of recorded variables by defining a reduced set of score variables that construct a Hotelling's T^2 statistic [21]. The mismatch between the recorded variables and their reconstruction using these score variables leads to the definition of the Q statistic [22]. The PCA method enables analysis of many sets of measurements simultaneously and facilitates the derivation of information to determine if the observed system is in an abnormal condition, with a level of confidence.

Similar to [17], the proposed islanding detection method is based on wide area phasor measurements, and is able to present a real-time wide-area view of islanding, and creates early warnings for system operators and engineers to maintain system security. This is motivated by the fact that one of the key findings of the August 2003 blackout in the U.S. and Canada was the lack of operator awareness during the time leading up to the blackout [23]. The more recent July 2012 Indian blackouts [24] further indicate the urgent need for the development of intelligent data analytical tools for wide area monitoring of *synchronized* PMU data to enhance real time situation awareness. In contrast to [17], in this study, an intelligent statistical approach based on PCA is introduced that enables the thresholds for event detection to be automatically determined based on long-term historic data. Moreover, the approach is simple to implement, computationally fast, provides a straightforward visualization; and has a simple geometrical interpretation. In addition, it can be used to detect when an islanded system is reconnected back to the transmission grid, and the contribution plots associated with PCA statistics can be used to identify the frequency variable which is affected by an islanding condition.

It is noted that similar work has been reported previously in [25], which attempted to apply PCA on PMU data including measurements of frequency, phase angle and voltage magnitude, but failed to perform islanding detection effectively. The previous method not only produced too many false alarms, but also the geometrical interpretation of islanding detection was lost. This is mainly caused by the underlying assumption of PCA, where the applied data should be linear and Gaussian distributed; however, both phase angle and voltage magnitude variables exhibit significant non-Gaussian characteristics for long-term historic data. Thus, in this paper, only frequency variables measured from different locations, which approximately follow a normal distribution, are considered. The proposed method has been able to correctly identify islanding events on the UK power system, as would be evident through visual inspection. To the best of our knowledge, this is the first research work that presents: (i) the successful application of the PCA method to real PMU data for islanding detection; (ii) an approach for geometrically interpreting islanding events and distinguishing them from other non-islanding events.

The paper is organized as follows. The relevant PCA-based statistical monitoring theory and related investigations for the wide area frequency measurements are presented next. Section III describes the real historic frequency data obtained from multiple locations on the UK power system for study, and gives results for the PCA applications. Discussion and conclusions are presented in Section IV and V, respectively.

II. Principal Component Analysis Based Islanding Detection

A. Principal Component Analysis of Wide Area Frequency Measurements

Principal component analysis, first proposed in 1901 [26], is one of the most popular multivariate dimension reduction techniques. It transforms a set of original correlated variables into a smaller set of uncorrelated ones [27]. These transformed variables are known as principal components, which are derived in the order of reducing variability with the first principal component accounting for the most significant variability in the original data [22]. The transformation can be viewed as an orthogonal rotation of the data such that maximum variation is projected onto the new axes, which are defined by the original

TABLE I
CALCULATION OF CONFIDENCE LIMITS FOR MONITORING STATISTICS

Statistic	Confidence Limit
$T^2 = \boldsymbol{t}^T \boldsymbol{\Lambda}^{-1} \boldsymbol{t}$	$\frac{r(N^2-1)}{N(N-r)} F_{r,N-r}$
$Q = \boldsymbol{e}^T \boldsymbol{e}$	$g \cdot \chi^2(h)$

variables. The correlations between the new variables will be removed after the rotation.

PCA identifies the orthogonal directions of maximum variance in the original data, by performing eigenvector/eigenvalue analysis of the sample covariance matrix. A more detailed description of PCA can be found in [22]. Liu *et al.* have previously applied PCA in statistical monitoring of a nuclear power plant waste management process for fault detection [28], and in wind farm oscillation monitoring [29]. This section gives a brief description of principal component analysis of frequency measurements for islanding detection.

Let $\mathbf{f} \in \mathbb{R}^m$ denote a sample vector storing m frequency variables. Assuming that there are N samples for each variable, a data matrix $\mathbf{F} \in \mathbb{R}^{N \times m}$ is composed with each row representing a sample. After scaling so that each column has zero-mean and unit variance, $\mathbf{F}$ can be decomposed into a score matrix $\mathbf{T} \in \mathbb{R}^{N \times r}$ and a loading matrix $\mathbf{U} \in \mathbb{R}^{m \times r}$ ($r \leq m$ is the number of retained principal components) [22]:

$$\mathbf{F} = \mathbf{T}\mathbf{U}^T + \mathbf{E} \tag{1}$$

where $\mathbf{E}$ is the residual matrix. A scaled sample vector $\mathbf{f}$ can be projected on the model subspace, which is spanned by $\mathbf{U}$, and the residual subspace, respectively [22].

The geometric simplicity of the PCA decomposition allows the construction of two univariate statistics, a Hotelling's T^2 statistic that represents significant variation of the recorded data and is associated with the PCA model plane and a Q statistic that describes the mismatch between the original variables and their projections onto the model plane, i.e. the variation of the data within the residual subspace. These two statistics, are defined as follows:

$$T^2 = \mathbf{f}^T \mathbf{U} \boldsymbol{\Lambda}^{-1} \mathbf{U}^T \mathbf{f} = \mathbf{t}^T \boldsymbol{\Lambda}^{-1} \mathbf{t} \tag{2}$$

and

$$Q = \mathbf{e}^T \mathbf{e} = \mathbf{f}^T \left[\mathbf{I} - \mathbf{U}\mathbf{U}^T \right] \mathbf{f} \tag{3}$$

where $\boldsymbol{\Lambda}$ is a diagonal matrix consisting of r eigenvalues of covariance matrix $\mathbf{S}$ of scaled $\mathbf{F}$. $\mathbf{t} = \mathbf{U}^T \mathbf{f}$ is a score vector, $\mathbf{e} \in \mathbb{R}^m$ is a residual vector and $\mathbf{I}$ represents an identity matrix. Under the assumption that the recorded variables are linear and normally distributed, the T^2 follows an F-distribution [22] and the Q statistic can be approximated by a central χ^2-distribution [21]. As discussed in [22], the confidence limits can be obtained as presented in Table I, where $g = \rho^2/2\mu$, $h = 2\mu^2/\rho^2$ and μ and ρ^2 are the sample mean and variance of the Q statistic.

For on-line wide area power system monitoring, a statistically significant number of violations of these limits, or at least one of them, is then indicative of abnormal system behavior.

B. A Geometric View of PCA-Based Islanding Detection

The theoretical basis of a geometric view of the PCA model is well explained in [21], [30]. Defining $\mathbf{z} = \boldsymbol{\Lambda}^{-1/2}\mathbf{t}$ and noting that $\mathbf{t} = \mathbf{U}^T\mathbf{f}$, the Hotelling statistic, $T^2 = \mathbf{z}^T\mathbf{z}$, can be viewed as a scaled squared 2-norm (or weighted distance) of an original frequency sample vector from its mean [21]. More specifically, the T^2 can be used to monitor system deviations from a target. When the weighted distance, represented by the T^2 statistic, is less than a confidence control limit, the system is considered to be on target.

For an original data set adequately explained by two principal components, the PCA model can be geometrically interpreted in 3 dimensions [30]. If the original data follow a multivariate normal distribution and represent the normal operating conditions, the data scatter can be enclosed in an ellipse whose axes are the principal component loadings [30]. The elliptical envelope is provided by the statistical confidence limit of the T^2 statistic, presented in Table I. If the system variables are highly correlated, the elliptical envelope becomes more elongated [21]. In addition, a third dimension is used to explain the deviation from the model plane, represented by the Q statistic [30].

When T^2 and Q statistics are utilized along with their respective confidence limits, it produces a cylindrical in-control region in 3-Dimensional (3-D) space for 3 variables explained by two principal components, as illustrated in Fig. 1. In the figure, the '$\times$'s represent data collected during in-control operation, while the '$\circ$'s and '+'s show data that violate the T^2 and Q statistic, respectively [21], [30].

Furthermore, the T^2 statistic in Eq. (2) represents the weighted distance (Mahalanobis distance) of any point from the target (e.g. 50 Hz for frequency variables in the UK power system). All points projected on the ellipse in the $t_1 - t_2$ plane in Fig. 1 would have the same value of T^2 statistic. Hence, a T^2 statistic chart would detect as a special event any point projected outside of the ellipse. In contrast to T^2, the Q statistic does not directly measure the variations along each eigenvector but measures the total sum of variations in the residual space. In another words, the Q statistic, also known as the squared prediction error, measures the deviation of the observations that was not captured by the PCA model. Using these two statistics together has been found to be effective at distinguishing between different types of faults in chemical process applications [21]. Here, a similar strategy is used in the power system context, to geometrically interpret islanding events (where the frequency variables deviate significantly from each other) and distinguish them from non-islanding events (where the frequency variables deviate from the target but do not deviate significantly from each other).

For the special case of monitored frequency variables recorded from different sites, a single principal component is sufficient to capture observed variability due to the high degree of correlation between variables. A geometric interpretation for islanding detection using the T^2 and the Q statistics of the PCA method can then be obtained in 2-Dimensional space (2-D) as demonstrated in Fig. 2. If the distance from the origin along the principal component line to the projected

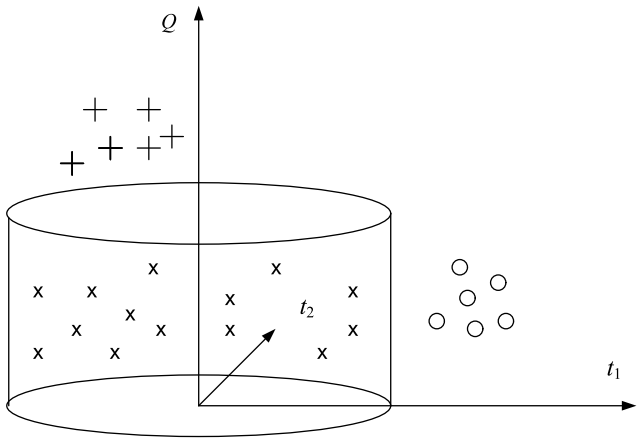

Fig. 1. A geometric interpretation for event detection using the T^2 and the Q statistics of PCA in 3-D. $\mathbf{t_1}$ and $\mathbf{t_2}$ are the first and the second principal components, respectively [21].

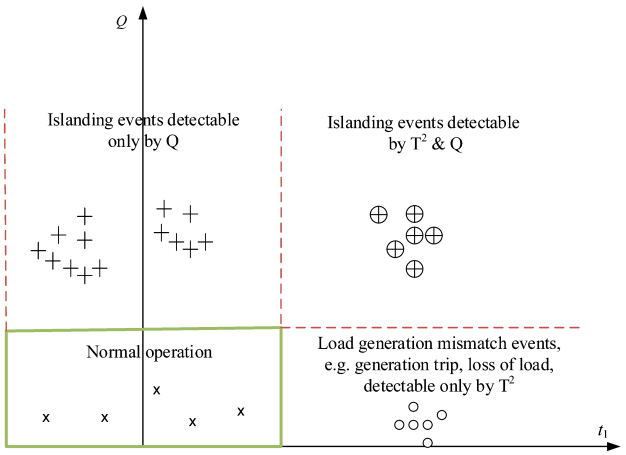

Fig. 2. A geometric interpretation for islanding detection using the T^2 and the Q statistics of the PCA method in 2-D.

data point is larger than the scaled maximum eigenvalue in the matrix $\mathbf{\Lambda}$, it will be detected by the T^2 statistic indicating that the frequency variables have significantly deviated from the target (50 Hz), i.e. a load and generation mismatch event has occurred. If the total sum of variations in the residual space violates the confidence value, it will be detected by the Q statistic indicating the frequency variables have deviated significantly from each other, i.e. an islanding event has occurred. This holds true due to the simple fact that the frequency variable is a universal parameter for the entire power grid. Essentially, as long as the data points are aligned with the first principal component direction ($y \approx x$, and the frequency variables are almost equal to each other) with a certain confidence limit, there is no significant deviation between the frequency variables. Otherwise, if data points are not aligned with the first principal component direction ($y \neq x$), then it indicates significant inter-frequency deviations (an islanding event occurs). This will be further demonstrated in the case studies presented later. Thus, in Fig. 2, the data points represented by '$\circ$' can only be detected by T^2, indicating global load and generation mismatch events where the frequency variables do not deviate significantly from each other. The data points represented by '+' can only be detected by Q and indicate islanding events where the frequency variables remain close to the target. Finally, the data points '$\oplus$' not only violate limits in the model space but also in the residual space (i.e. they are detected by both T^2 and Q), and hence they indicate islanding events where the frequency variables have deviated significantly from each other and from the 50 Hz target.

C. Contribution Plots of Monitored Frequency Variables to PCA Statistics

Contribution plots identify the contribution of individual frequency variables to the PCA statistics. If the contribution of a particular frequency variable towards the Q statistic is large, an islanding site can be identified. The contribution of the ith frequency variable to the Q statistic can be obtained as follows:

$$Q_{CONT} = \mathbf{\Phi}_i^T \mathbf{f} \tag{4}$$

where $\mathbf{\Phi}_i^T$ is the ith row of the matrix $\mathbf{I} - \mathbf{U}\mathbf{U}^T$. The variable contribution to the T^2 statistic, defined in [31], can be used to determine if the monitored frequency variable deviates significantly from its target.

In summary, the implementation of the proposed PCA-based islanding detection method involves two steps: 1) off-line PCA modelling using historic data to obtain the principal components and control limits; and 2) on-line monitoring to determine if an islanding event occurs. Further details of the proposed islanding detection strategy are provided in Fig. 3.

III. UK Power System Case Study

A. UK Power System Wide Area Phasor Data

In the UK power grid, a type of single-phase phasor measurement unit, developed at Queen's University Belfast (QUB) as part of the OpenPMU project [32], [33] is installed at sites of interest for islanding detection, including embedded generation (at 415 V) and main distribution substations (33 kV). The PMUs report at 10 Hz and measurements of frequency, voltage magnitude, and voltage phase angle are sent via the Internet to a server at QUB for analysis. The locations of the units are highlighted in Fig. 4. The units used in this study are supported by Scottish and Southern Energy Ltd.

From the UK power system, 7 days of recorded historic data from 6 sites was used as reference data to determine the relevant normal operational statistics. The data set consisted of a total of 5,446,101 synchronous multivariate samples (with 601,899 samples missing). The histogram plot of the frequency, phase angle difference and voltage magnitude along with its corresponding normal distribution curve and kernel density estimate, is shown in Fig. 5. It is clear that the frequency variable approximately follows a normal distribution, while the others demonstrate significant non-Gaussian characteristics. Due to the limited space, only the frequency variable is analyzed here. More advanced approaches will be applied to phase angle difference and voltage data in our future work, to address the non-Gaussian related issues.

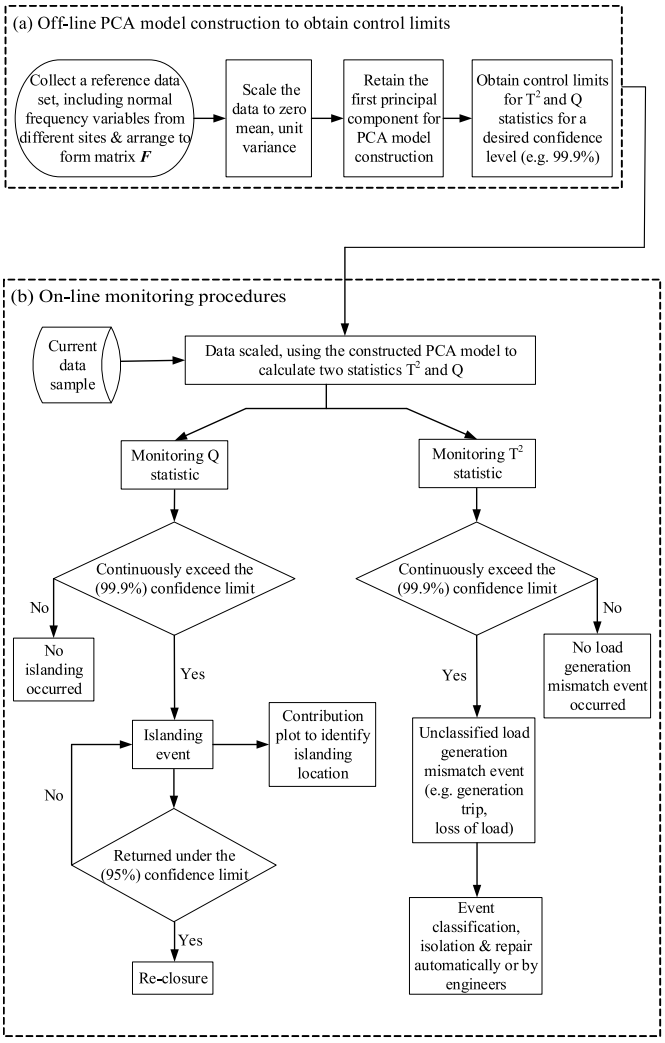

Fig. 3. Flow chart of the proposed PCA method for islanding detection.

TABLE II
VARIANCE CONTRIBUTION OF PRINCIPAL COMPONENTS (PCS)

#PC(s)	Percent Variance Captured by PCA Model	
	Eigenvalue of Cov(**F**)	Variance Captured %
1	5.969	99.48
2	0.011	0.18
3	0.007	0.12
4	0.006	0.11
5	0.006	0.09
6	0.001	0.02

B. PCA Modelling

The reference data set of the frequency variables from 6 sites (f_1 - Southern England, f_2 - Manchester, f_3, f_4, f_5, f_6 - Orkney Islands) were used to produce a covariance matrix. The eigenvalues of the covariance matrix and the contribution of each principal component to the reconstruction of the original data are summarized in Table II.

As expected, the first principal component corresponding to the largest eigenvalue, captures 99.48% of the total variance, and as such represents the significant system variation and the interrelationships between the six frequency variables

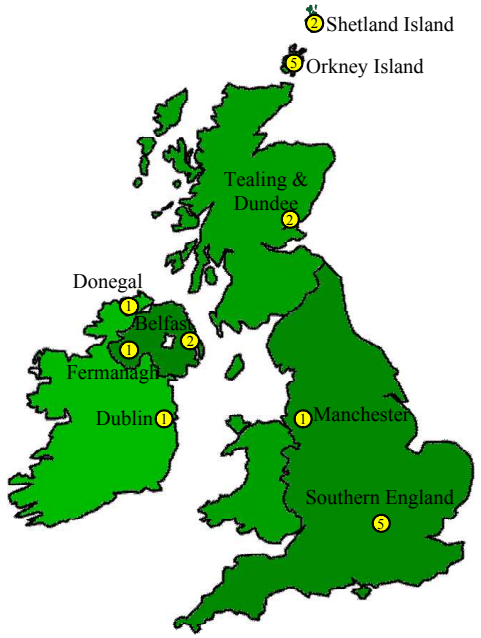

Fig. 4. OpenPMU Layout in the UK System, revised from [32]. The numbers in the circles are the number of PMUs installed at the associated locations.

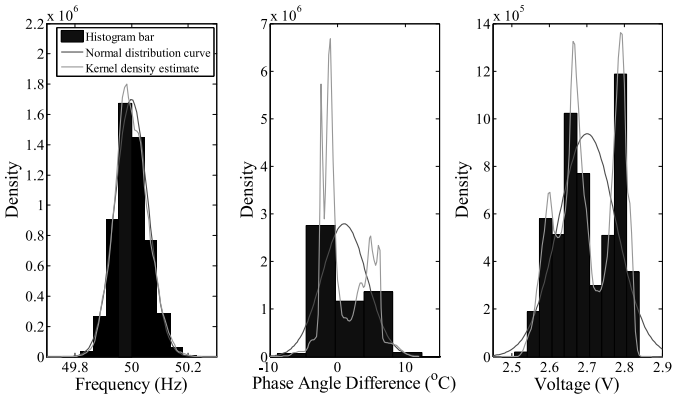

Fig. 5. Histogram plot of frequency, phase angle difference, and voltage magnitude, along with its corresponding normal distribution curve, and kernel density estimate.

collected from different locations in the power grid, whilst the remaining five components capture the noise variance [21]. This agrees with the scatter plot of the frequency variables of the reference data set, shown in Fig. 6. Thus only the first principal component is used to construct the PCA model. In addition, for the 5,446,101 synchronous multivariate reference data, the Type I error, or the false alarm rate, from the T^2 and Q statistics of the PCA model for a confidence of 99.9% are 0.14% and 0.13%, respectively. This implies that the Type I errors for the T^2 and the Q statistics are close to the expected 0.1%.

In the following, two real case studies including one with both inter-connector trip and islanding events, and the other with loss of load, inter-connector trip and islanding events, are presented to verify the proposed PCA method for islanding detection.

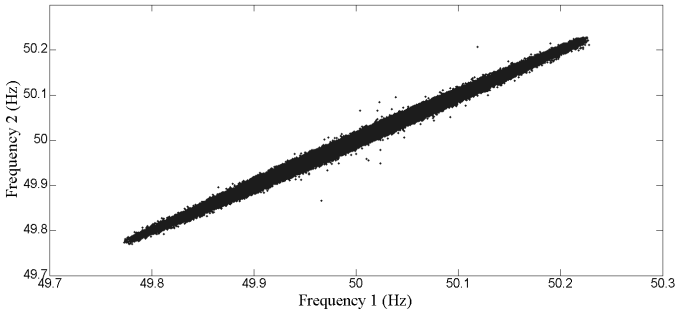

Fig. 6. Frequency scatter plot of frequency 1 (f_1) and frequency 2 (f_2).

C. Case 1: Inter-connector Trip and Islanding Events on 28/09/2012

1) Islanding Detection: On 28 September 2012 a inter-connector trip event occurred between Great Britain (GB) and France, which resulted in an instantaneous loss of 1 GW being imported to the GB power grid. In the 10 seconds after the loss, the frequency of the main power system fell from 50.08 Hz to 49.70 Hz. The resulting rate-of-change of frequency -0.186 Hz/second (calculated over 50 cycles) at the north of the UK exceeded the current RoCoF setting of -0.125 Hz/second recommended by the UK Grid Code G59/2 [34], which falsely triggered an islanding operation on the PMU site, located at a MV substation and lead to the further loss of embedded generation.

The frequency plot of test data recorded at the 6 sites for 28 September 2012, including a magnified view of the event, is shown in Fig. 7 (a). As can be observed, the inter-connector tripped at 02:48:37, and an island occurred immediately after the generation loss and lasted nearly 5 hours. The frequency scatter plot for case 1 is depicted in Fig. 7 (b). When the inter-connector trip events occurs, some data points are dragged further away from the reference data, in the model space as well as in the residual space, i.e. along the direction of the T^2 as well as that of the Q.

The PCA-based monitoring result for case 1 is illustrated in Fig. 8. As can be seen, the islanding event has been successfully detected by the Q statistic from 02:48:38 to 07:42:01. In addition, the T^2 statistic detected that the frequency variable violated its control limit at 02:48:39 and 08:03:29, both corresponding to generation dip events. A confidence limit of 99.9% is employed to avoid excessive false alarms.

To check islanding detection accuracy and response time, Fig. 9 shows the close-up of both the frequency plot and the PCA monitoring result for the data from 02:48:36 to 02:48:43, where the inter-connector trip events occurred. It is clear that the Q statistic detected the islanding event immediately after it occurred from 02:48:38 without any delay (enclosed by the red elliptical line). It should be noted that for the first 500 ms the frequency deviation in the Q statistic is caused by measurement error or transient phenomena due to the inter-connector trip. In practice, a 500 ms islanding detection delay is deliberately introduced, to avoid false triggers. It is clear that the T^2 statistic (upper plot, Fig. 9 (b)) detected a frequency deviation from its target (50 Hz) at 02:48:39

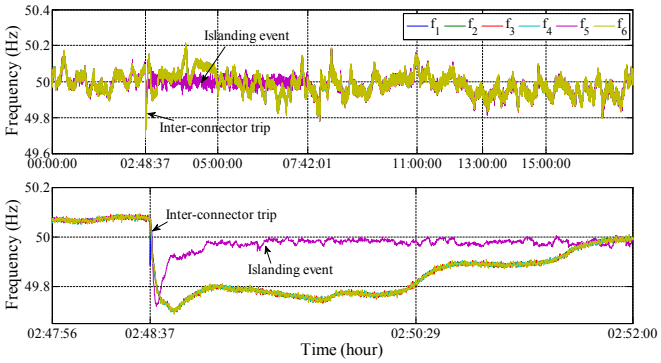

(a) Frequency plot

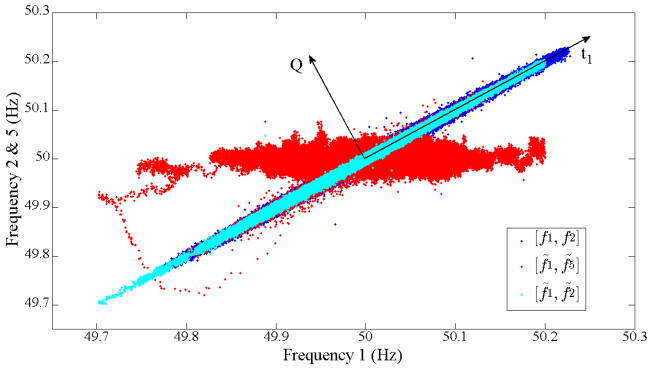

(b) PCA results

Fig. 7. Case 1 on 28/09/2012. (a) Frequency plot (upper plot); Close up of frequency plot (lower plot) (b) A 2-D illustration of the test data. The blue dot represents the reference data $[f_1, f_2]$, the red dot and the cyan dot represent the test data $[\tilde{f}_1, \tilde{f}_5]$ and $[\tilde{f}_1, \tilde{f}_2]$, respectively. When the inter-connector trip occurs, some points drag further away from the reference data, along the principal component direction t_1 as well as the Q direction.

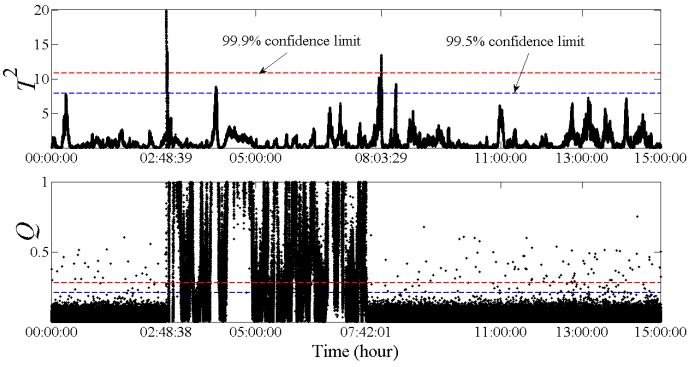

Fig. 8. PCA monitoring results for case 1.

(enclosed by the cyan elliptical line). Further study revealed that the contribution of islanding event to T^2 was from 02:48:39 and lasted only 3 seconds, while the contribution of non-islanding events to T^2 was from 02:49:40 and lasted for about 2 minutes.

2) Return-to-mains Detection: Fig. 10 shows the magnified frequency plot and PCA monitoring result for data from 07:40:10 to 07:43:07, in which the islanding site returned to mains. It is clear that the Q statistic detected the re-closure from 07:42:01 at the 95% confidence limit. It is observed that from 07:41:04 to 07:42:01 the frequency deviation of the

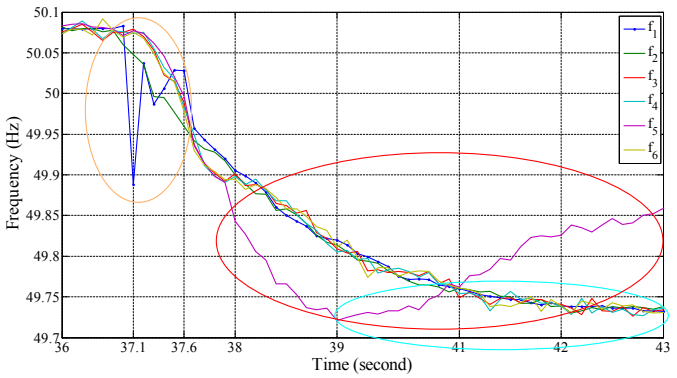

(a) Frequency plot

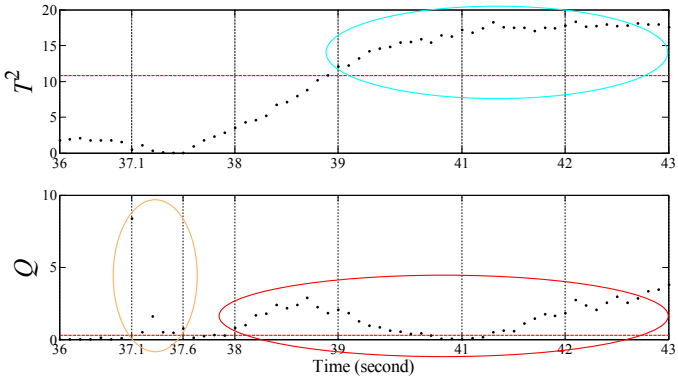

(b) PCA results

Fig. 9. Close up of: (a) frequency plot; (b) PCA monitoring results of case 1 for data from 02:48:36 to 02:48:43, including islanding and generation trip on 28/09/2012.

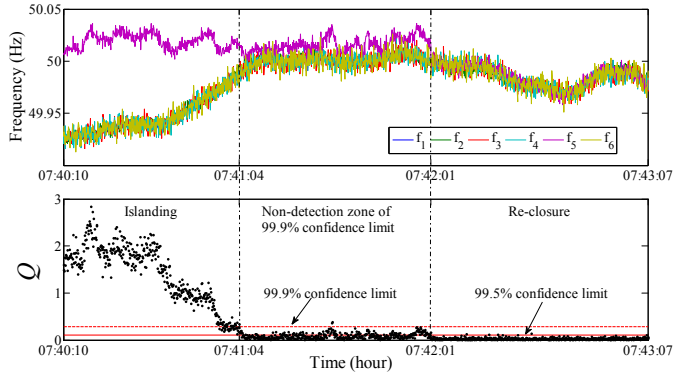

Fig. 10. Close up on frequency plot of re-closure for case 1 on 28/09/2012, for data from 07:40:10 to 07:43:07 (upper plot); PCA monitoring results (lower plot).

islanding site (the purple line) from the other sites is less than 0.03 Hz (upper plot in Fig. 10) and the islanding event remains in the non-detection zone of the 99.9% confidence limit (lower plot in Fig. 10). To improve the confidence of return-to-mains detection, the confidence limit was switched to 95%.

3) Contribution Plot for Islanding Location Identification: Fig. 11 shows the variable contributions to the Q statistic (lower plot) and the T^2 statistics (upper plot) at 02:48:45. The variable that significantly contributed to the Q statistic of the PCA model was identified as the fifth frequency variable,

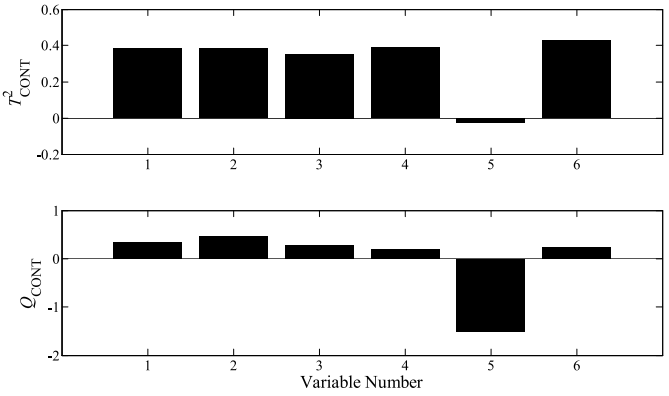

Fig. 11. Contribution plot to T^2 (upper plot) and Q statistics (lower plot) for case 1

indicating the islanding site location as the Orkney Islands, which is in the north of the UK. This simple graphical representation would help the system operator identify and pinpoint the islanding location, or locations immediately after occurrence. Areas that form part of the same synchronous island could be quickly and accurately determined. In case 1, based on the fact that f_3, f_4, f_5 and f_6 were recorded from 4 PMUs at the Orkney Islands, f_3, f_4 and f_6 were synchronized with the main grid (f_1 and f_2), and f_5 was recorded from a PMU site located at a MV substation, the islanding location can be narrowed down to a 33 kV substation.

In addition, Fig. 11 also shows that the contribution of the fifth variable to the T^2 statistic is low, indicating that the frequency of the islanding site hasn't deviated significantly from the target frequency (50 Hz) at this time instant.

D. Case 2: Loss of Load, Inter-connector Trip and Islanding Events on 30/09/2012

The 30 September 2012 saw a high frequency event at 02:28 in the morning, followed by a low frequency event in the evening at 15:03. The high frequency event was due to loss of load. The low frequency event was again due to a fault on the GB-France power import, with a subsequent loss of 1 GW to the GB power system. In the later low frequency event the frequency fell from 49.97 Hz to 49.6 Hz in 10 seconds after the inter-connector loss. The rate-of-change of frequency at the north of UK was -0.155 Hz/second (calculated over 50 cycles) and again exceeded the current RoCoF setting of -0.125 Hz/second erroneously triggering islanding protection leading to further loss of embedded generation. These high and low frequency events (corresponding to loss of load and generation dip, respectively), are again used to examine the effectiveness of the proposed method. As shown in Fig. 12, the Q statistic (middle plot) successfully detected the islanding event at 15:03:30. Further examination revealed this islanding event, lasted for about 9 minutes. The T^2 statistic (upper plot) in Fig. 12, however, detected the generation dip event also at 15:03:30. This agrees with the frequency scatter plot in Fig. 13, where the islanding event is clearly represented by the red dots which deviate from the reference data along the Q

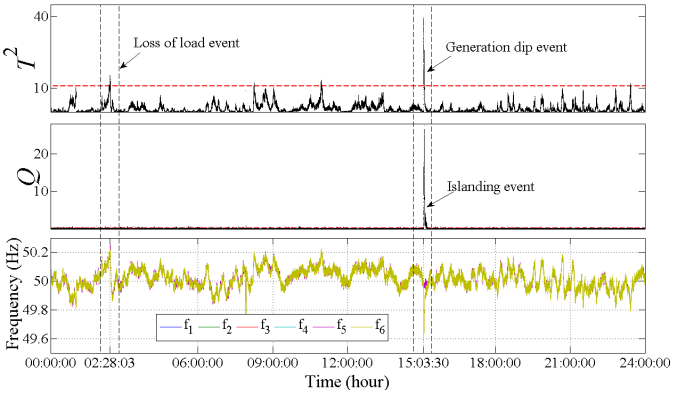

Fig. 12. PCA monitoring results (upper plot for the T^2 and middle plot for the Q statistic) and frequency plot (Lower plot) for case 2 on 30/09/2012.

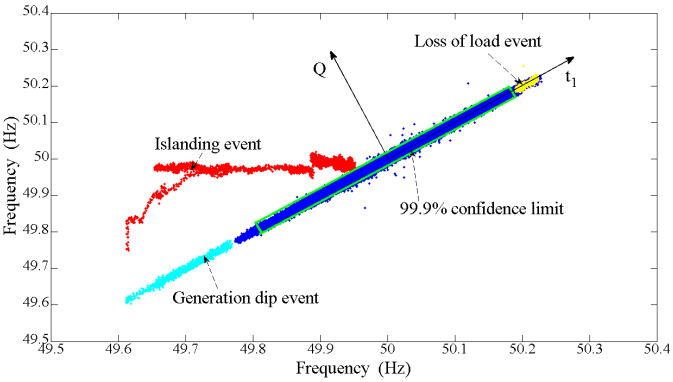

Fig. 13. 2-D illustration for the islanding detection. The blue/cyan/red/yellow dot represents the reference data/generation dip/islanding/load shedding event, respectively.

direction, and the generation dip events is represented by the cyan dots which violate the reference data along, and only along, the principle component i.e. the T^2 direction.

It should be noted that another frequency deviation event was detected by the T^2 statistic at 02:28:03 for 1.5 minutes, which corresponds to the loss of load event in Fig. 13. This further demonstrated that the proposed PCA method was able to detect islanding events accurately, but also able to prevent false triggering caused by the generation dip and loss of load events, where the frequencies do not deviate from each other.

IV. Discussion

As illustrated in the flow chart in Fig. 3, the proposed PCA based islanding detection method, involves off-line PCA modelling and on-line monitoring. The implementation of the proposed method requires consideration of a number of issues:

1) Response time. The detection time for the proposed method will have a time delay, calculated as $T = T_{cal}+T_D+T_{com}$, where T_{cal} is the computation time of the proposed algorithm and in most cases is negligible, T_D is the introduced time delay of 500 ms, to avoid false triggering by measurement error etc., and T_{com} is the latency of two-way communication, which is normally between 20 and 200 ms depending on design [32], [33]. In general, a response time of less than 2 seconds can be achieved meeting the IEEE standard [18]. If the communication link is down or communication latencies are high, local approaches can be used as back-up solutions.
2) Detectability. It should be noted that if the frequency in the islanding system is well matched with those of other sites, our approach will fail to detect islanding successfully. More advanced approaches, will be applied to other variables, such as voltage phase angle, and used as a complementary method.
3) Scalability. The proposed methodology is targeted at presenting a real-time wide area view of system islanding and creating early warnings for system operators. However, the methodology can also be used as a local or regional approach, where multiple sites are used to provide a much more secure reference signal. This includes using other nearby distributed generator sites connected to the same substation and using the same protection scheme to determine islanding by consensus, perhaps being able to trip a particular distributed generator that fails to detect, or avoid a nuisance trip. It should be noted that islanding can also occur in transmission systems. The proposed approach is generic and also useful for this situation.
4) Observability. The accuracy of islanding detection and location is highly dependent on the topology of the PMU layout and the prior knowledge of the investigated network. To ensure full network observability, optimal PMU placement will be further investigated.

The proposed methodolgy was applied to PMU data from the UK power network, which had an average distributed generation (DG) penetration of over 11% in 2012 [35]. The examined local network situated in the Orkney Islands often exports power, reflecting 100% distributed renewable energy penetration in this area [36]. The case studies presented demonstrate that the proposed methodology is a promising approach to islanding detection. The scalability of the approach makes it an attractive proposition for networks with high penetration of DG, where there is an increased risk of uncontrolled islanding operation. In addition, its dependence on frequency rather than voltage magnitude makes it insensitive to local voltage problems that can be an issue [37] with DG. Overall, the relative simplicity and statistical basis of the approach make it a powerful tool for real time situation awareness that could aid system operators in preventing large scale blackouts should islanding situations occur.

V. Conclusion

This paper presents a multivariate statistical methodology for analysing wide area synchronized frequency measurements for islanding detection. Using principal component analysis, it is shown that the Q statistic is able to discriminate islanding events from other grid disturbances, such as inter-connector trip, generation dip/trip and loss of load events. The advantages of the proposed approach when compared with the conventional RoCoF technique and the newly proposed frequency

difference method [17] are: (1) the threshold for islanding detection can be automatically determined based on long-term historic data; (2) it is simple to implement, computationally fast with straightforward visualization; (3) it can be used to detect islanding system re-closure; (4) associated contribution plots can identify the islanded site, sites and regions; (5) in addition, the T^2 statistic is able to detect frequency deviation events, such as loss of load and generation trip.

The limitation of this approach is that if the frequency in the islanding system is well matched with those of other sites, it will fail to detect islanding successfully. In addition, incomplete data and outliers are also challenging problems for its practical use. More advanced approaches, such as non-Gaussian, probabilistic, and recursive approaches will be investigated and applied to other variables in our future work aiming to improve detectability robustness.

ACKNOWLEDGMENT

The authors would like to thank Prof. Y. S. Xue from State Grid Electric Power Research Institute of China for the useful discussions during his visit to Queen's University Belfast. Valuable discussions with Dr. J. Kennedy from System Operator Northern Ireland and Prof. L. Xie from Zhejiang University, are also acknowledged. In addition, the authors wish to thank the reviewers for their comments.

REFERENCES

[1] "A strategic energy framework for Northern Ireland," Department of Enterprise, Trade, and Investment, Northern Ireland, UK, http://www.detini.gov.uk/, 2010.

[2] E. Martinot and J. Li, "Worldwatch report: Powering china's development," Tech. Rep., 2007.

[3] W. Freitas, W. Xu, C. Affonso, and Z. Huang, "Comparative analysis between ROCOF and vector surge relays for distributed generation applications," *IEEE Trans. Power Del.*, vol. 20, no. 2, pp. 1315–1324, 2005.

[4] N. W. A. Lidula and A. Rajapakse, "A pattern-recognition approach for detecting power islands using transient signals - part ii: Performance evaluation," *IEEE Trans. Power Del.*, vol. 27, no. 3, pp. 1071–1080, 2012.

[5] S. R. Samantaray, K. El-Arroudi, G. Joos, and I. Kamwa, "A fuzzy rule-based approach for islanding detection in distributed generation," *IEEE Trans. Power Del.*, vol. 25, no. 3, pp. 1427–1433, 2010.

[6] W. Najy, H. Zeineldin, A. Alaboudy, and W.-L. Woon, "A Bayesian passive islanding detection method for inverter-based distributed generation using esprit," *IEEE Trans. Power Del.*, vol. 26, no. 4, pp. 2687–2696, 2011.

[7] P. Mahat, Z. Chen, and B. Bak-Jensen, "Review on islanding operation of distribution system with distributed generation," in *Proc. IEEE Power Energy Soc. Gen. Meeting*, 2011, pp. 1–8.

[8] M. Redfern, J. I. Barrett, and O. Usta, "A new microprocessor based islanding protection algorithm for dispersed storage and generation units," *IEEE Trans. Power Del.*, vol. 10, no. 3, pp. 1249–1254, 1995.

[9] F.-S. Pai and S.-J. Huang, "A detection algorithm for islanding-prevention of dispersed consumer-owned storage and generating units," *IEEE Trans. Energy Convers.*, vol. 16, no. 4, pp. 346–351, 2001.

[10] M. Sumner, B. Palethorpe, D. W. P. Thomas, P. Zanchetta, and M. Di Piazza, "A technique for power supply harmonic impedance estimation using a controlled voltage disturbance," *IEEE Trans. Power Electron.*, vol. 17, no. 2, pp. 207–215, 2002.

[11] D. Reigosa, F. Briz, C. Charro, P. Garcia, and J. Guerrero, "Active islanding detection using high-frequency signal injection," *IEEE Trans. Ind. Appl.*, vol. 48, no. 5, pp. 1588–1597, 2012.

[12] M. Ropp, M. Begovic, and A. Rohatgi, "Analysis and performance assessment of the active frequency drift method of islanding prevention," *IEEE Trans. Energy Conversion*, vol. 14, no. 3, pp. 810–816, Sep 1999.

[13] N. W. A. Lidula, N. Perera, and A. Rajapakse, "Investigation of a fast islanding detection methodology using transient signals," in *Proc. IEEE Power Energy Soc. Gen. Meeting*, 2009, pp. 1–6.

[14] K. El-Arroudi, G. Joos, I. Kamwa, and D. McGillis, "Intelligent-based approach to islanding detection in distributed generation," *IEEE Trans. Power Del.*, vol. 22, no. 2, pp. 828–835, 2007.

[15] K. El-Arroudi and G. Joos, "Data mining approach to threshold settings of islanding relays in distributed generation," *Power Systems, IEEE Transactions on*, vol. 22, no. 3, pp. 1112–1119, 2007.

[16] P. E. A. Etxegarai and I. Zamora, "Analysis of remote islanding detection methods for distributed resources," in *Int. Conf. Renew. Energies Power Quality*, Las Palmas de Gran Canaria, Spain, 2011.

[17] Z. Lin, T. Xia, Y. Ye, Y. Zhang, L. Chen, Y. Liu, K. Tomsovic, T. Bilke, and F. Wen, "Application of wide area measurement systems to islanding detection of bulk power systems," *IEEE Trans. Power Syst.*, vol. 28, no. 2, pp. 2006–2015, May 2013.

[18] *Standard for Interconnecting Distributed Resources With Electric Power Systems*. IEEE Std. 1547, 2003.

[19] *Photovoltaic (PV) systems - Characteristics of utility interface*. IEC Std. 61727, 2004.

[20] J. Thambirajah, N. Thornhill, and B. Pal, "A multivariate approach towards interarea oscillation damping estimation under ambient conditions via independent component analysis and random decrement," *IEEE Trans. Power Syst.*, vol. 26, no. 1, pp. 315–322, 2011.

[21] C. L. Russell, E.L. and R. Braatz, *Data-driven Methods for Fault Detection and Diagnosis in Chemical Processes*. New York: Springer-Verlag, 2000.

[22] J. E. Jackson, *A Users Guide to Principal Components*, ser. Wiley Series in Probability and Mathematical Statistics. New York: John Wiley, 1991.

[23] P. Myrda and K. Donahoe, "The true vision of automation," *IEEE Power Energy Mag.*, vol. 5, no. 3, pp. 32–44, 2007.

[24] P. Pentayya, A. Gartia, S. Saha, R. Anumasula, and C. Kumar, "Synchrophasor based application development in Western India," in *Proc. IEEE Innovative Smart Grid Technologies Asia*, 2013, pp. 1–6.

[25] Y. J. Guo, K. Li, and D. Laverty, "A statistical process control approach for automatic anti-islanding detection using synchrophasors," in *Proc. IEEE Power Energy Soc. Gen. Meeting*, 2013, pp. 1–5.

[26] C. Pearson, "On lines and planes of closest fit to systems of points in space," *Phil. Mag., Series B.*, vol. 2, no. 11, pp. 559–572, 1901.

[27] C. Chatfield and A. Collins, *Introduction to Multivariate Analysis*. London: Chapman and Hall/CRC, 1981.

[28] X. Liu, L. Xie, U. Kruger, T. Littler, and S. Wang, "Statistical-based monitoring of multivariate non-Gaussian systems," *AIChE J.*, vol. 54, no. 9, pp. 2379–2391, 2008.

[29] X. Liu, D. McSwiggan, T. Littler, and J. Kennedy, "Measurement-based method for wind farm power system oscillations monitoring," *IET Renew. Power Gen.*, vol. 4, no. 2, pp. 198–209, 2010.

[30] A. Raich and A. Çinar, "Statistical process monitoring and disturbance diagnosis in multivariable continuous processes," *AIChE J.*, vol. 42, no. 4, pp. 995–1009, 1996.

[31] T. Kourti and J. F. MacGregor, "Multivariate SPC methods for process and product management," *J. Qual. Technol.*, vol. 28, pp. 409–428, 1996.

[32] D. Laverty, D. Morrow, R. Best, and M. Cregan, "Anti-islanding detection using synchrophasors and internet protocol telecommunications," in *Proc. 2nd IEEE PES Int. Conf. Exhib. ISGT Europe*, 2011, pp. 1–5.

[33] D. Laverty, R. Best, P. Brogan, I. Al Khatib, L. Vanfretti, and D. Morrow, "The openpmu platform for open-source phasor measurements," *IEEE Trans. Instrum. Meas.*, vol. 62, no. 4, pp. 701–709, 2013.

[34] *Recommendations for the Connection of Generating Plant to the Distribution Systems of Licensed Distribution Network Operators*. ER G59/2, 2010.

[35] "UK renewable energy roadmap update 2012," Department of Energy & Climate Change, https://www.gov.uk/, 2012.

[36] R. Currie, D. MacLeman, G. McLorn, and R. Sims, "Operating the orkney smart grid: practical experience," in *Proc. 21th Int. Conf. Elect. Dis., CIRED*, 2011, pp. 1–4.

[37] P.-C. Chen, R. Salcedo, Q. Zhu, F. de Leon, D. Czarkowski, Z.-P. Jiang, V. Spitsa, Z. Zabar, and R. Uosef, "Analysis of voltage profile problems due to the penetration of distributed generation in low-voltage secondary distribution networks," *IEEE Trans. Power Del.*, vol. 27, no. 4, pp. 2020–2028, 2012.